The Journal of Chemical Physics

RESEARCH ARTICLE | MARCH 27 2023

Orientation and dynamics of water molecules in beryl

Vojtěch Chlan ; Martin Adamec ; Helena Štěpánková ; Victor G. Thomas ; Filip Kadlec

J. Chem. Phys. 158, 124308 (2023)
https://doi.org/10.1063/5.0131510

The Journal of Chemical Physics ARTICLE scitation.org/journal/jcp

Orientation and dynamics of water molecules in beryl

Cite as: J. Chem. Phys. 158, 124308 (2023); doi: 10.1063/5.0131510
Submitted: 21 October 2022 • Accepted: 7 March 2023 •
Published Online: 27 March 2023

Vojtěch Chlan,[1,a)] Martin Adamec,[1,2] Helena Štěpánková,[1] Victor G. Thomas,[3] and Filip Kadlec[2]

AFFILIATIONS

[1] Charles University, Faculty of Mathematics and Physics, Department of Low Temperature Physics, V Holešovičkách 2, 180 00 Prague 8, Czech Republic
[2] Institute of Physics of the Czech Academy of Sciences, Na Slovance 2, 182 00 Prague 8, Czech Republic
[3] V.S. Sobolev Institute of Geology and Mineralogy SB RAS, 630090 Novosibirsk, Russia

[a)] **Author to whom correspondence should be addressed:** vojtech.chlan@mff.cuni.cz

ABSTRACT

Behavior of individual molecules of normal and heavy water in beryl single crystals was studied by ^{1}H and ^{2}H nuclear magnetic resonance spectroscopy. From temperature dependences of the spectra, we deduce that type-I water molecules embedded in the beryl voids are oriented quite differently from the view established in the literature: Different from the earlier assumptions, their H–H lines deviate by about 18° from the hexagonal axis. We suggest that this is due to the molecules attaching to the oxygen atoms forming the beryl structural voids by a hydrogen bond. Our analysis shows that the molecules perform two types of movement: (i) rapid librations around the axis of the hydrogen bond and (ii) less frequent orientational jumps among the 12 possible binding sites in the beryl voids. The frequencies of the librational motions are evaluated from a simple thermodynamic model, providing good quantitative agreement with the frequencies of librations from optical experiments reported earlier.

I. INTRODUCTION

A. Water confined in beryl

Water confined in nanoscale volumes manifests many unusual properties and has recently drawn a considerable attention. Among the known corresponding structures, hydrated beryl $Be_3Al_2Si_6O_{18}$ is a system attracting a broad interest where tendencies to low-temperature ferroelectric ordering of the crystal water were clearly demonstrated.[1,2] In fact, the water molecules can occupy regularly spaced crystal sites enclosed by oxygen atoms (see Fig. 1). These sites define well the molecules' positions; in contrast, their angular orientations are generally variable. Note also that, as a rule, only a partial beryl hydration is achieved. Thus, in this system, unlike in common condensed phases of water, hydrogen bonding among the water molecules is suppressed, and they interact predominantly via electric dipole–dipole interactions involving their dipole moments of 1.85 D ($6.17 \cdot 10^{-30}$ C m). Incipient ferroelectricity has been documented especially by observations of collective vibrations of the water molecules, producing a ferroelectric soft phonon mode. This soft mode was observed in the THz-range spectra of dielectric permittivity, obeying the usual Curie–Weiss and Cochran temperature dependences.[2] In the reported case, a negative Curie temperature of $T_C \approx -20$ K was determined, so no ferroelectric state could be achieved. Additionally, at temperatures below about 20 K, the phonon no more softened; instead, its frequency was leveling off, which has been attributed to quantum tunneling.[3,4] For the above reasons, hydrated beryl has been one of the most studied crystal systems featuring confined water.[1–7] Owing to its well-defined geometry and interesting observed phenomena, hydrated beryl can serve as a model structure for more detailed spectroscopic and theoretical studies, with the aim of improving the current knowledge of the underlying phenomena, which may favor or suppress the ordering of confined water molecules.

The crystal structure of beryl is hexagonal (space group $P6/mcc$), and it contains channels of voids running along its hexagonal axis. Each of these voids may accommodate one water molecule. For more than fifty years, the water molecules have been supposed to take up two possible types of orientations within the voids, as hypothesized first by Wood and Nassau based on their infrared spectra analysis.[10] They concluded that the molecules will orient

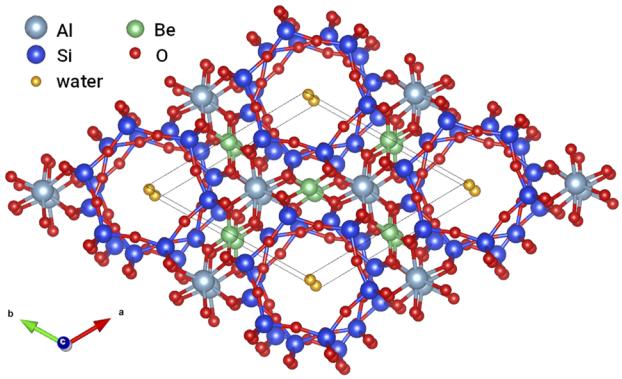

FIG. 1. View of the crystal structure of beryl along the hexagonal axis *c*. The thin lines denote the unit cell whereas the yellow circles indicate the possible positions of the water molecules within the structural voids. The structural data[8] were visualized using the Vesta software.[9]

themselves with the H–H lines oriented either parallel to the hexagonal axis ("type-I water") or perpendicular to it ("type-II water"); the latter type should be present especially in crystals with an additional doping, as the oxygen may bind to an impurity atom located within the channel. The earlier studies dealing with the interactions among the water molecules and their collective dynamics assumed the type-I molecules to rotate around the hexagonal axis of beryl, so the molecules' planes remained parallel to the hexagonal axis. At the same time, it was supposed that the molecules are subjected, in their angular orientations, to a local potential exhibiting six equivalent minima separated by angles of 60°.[3–6,11] Whereas the properties of the molecular ensemble were studied quite extensively—see the above references—the orientations and dynamics of the individual molecules in the voids have been still less explored, despite being crucial for the bulk properties. Such local, molecular-level information can be provided by nuclear magnetic resonance (NMR) spectroscopy.

B. NMR spectroscopy of water in beryl

Water molecules are expected to produce a single peak in the ^{1}H NMR spectrum because the spin of the ^{1}H nucleus (proton) is $\frac{1}{2}$ and both hydrogen atoms are equivalent due to symmetry. The peak may become split and/or shifted when anisotropic interactions are involved, e.g., dipolar interactions or anisotropy of chemical shielding. In cases when the water molecules are highly mobile, such as in liquid or gas phases, the effect of these anisotropic interactions on the NMR spectrum gets averaged by the fast molecular reorientations (*motional narrowing*). Then, the ^{1}H nuclei in water molecules are exposed to the same, averaged local fields and the ^{1}H NMR spectrum of water consists of a single, usually very narrow peak.[12]

Water molecules in solids have their dynamics significantly restricted. When the molecules are static or their reorientations are very slow (e.g., in ice or as a water of crystallization), the anisotropic interactions are not fully averaged and the NMR spectrum comprises contributions from all arrangements of the molecule present in the sample. For single crystals, the NMR spectra depend on the crystal orientation with respect to external magnetic field $\mathbf{B}_0$, while the NMR spectra of powders with randomly oriented grains display powder-pattern features.[12] In terms of magnitude, the anisotropy of chemical shielding of ^{1}H in water molecule ranges from 19 to 35 ppm for various phases of water,[13] which for $B_0 \sim 10$ T corresponds to shifts or splittings of peaks in the ^{1}H spectrum of about 10 kHz. The effect of dipolar interactions between ^{1}H nuclei within the water molecule may be an order of magnitude larger, the dipolar interaction is thus often the dominant source of anisotropy in ^{1}H NMR spectra of solids.[12]

The character of the ^{1}H NMR spectrum of water molecules enclosed in the crystal voids is different from the two cases presented above. The confined molecules are not static as in ice, and the molecular reorientations are not isotropic as in liquid water. Thus, the anisotropic interactions are not fully averaged and the ^{1}H NMR spectrum of water consists of more than one peak. This is the case of water molecules confined in the voids of beryl crystal, which was first studied using NMR in the work of Paré and Ducros[14] and in the work of Sugitani *et al.*[15] already in 1960s. In both these works, the ^{1}H NMR spectra comprise doublet of peaks arising due to the nuclear dipolar interaction between the ^{1}H nuclei within the water molecules. The signal was attributed to type-I water. Moreover, the observed dipolar splitting increased linearly with decreasing temperature and saturated below 100 K. The natural interpretation then was that the water molecules oscillate around their equilibrium positions when H–H line is parallel to the hexagonal axis and that the amplitudes of oscillations increase with temperature.[14]

However, the idea that the type-I water molecules are simply oscillating around the hexagonal axis is not entirely correct since even at the lowest temperatures, the observed dipolar splitting does not reach the expected value, which is precisely given by the distance between the ^{1}H nuclei within the water molecule. As we show in this paper, the movements of water molecules must be more complex. This deduction is based on measuring and analyzing the dipolar splitting in ^{1}H NMR quantitatively and especially by measuring and analyzing ^{2}H NMR in beryl hydrated by heavy water.

The spin quantum number of the ^{2}H nucleus equals 1 and so, in the presence of an external magnetic field, two transitions between the nuclear energy levels of the Zeeman multiplet are observable. Thus, the ^{2}H NMR spectrum of heavy water in beryl is expected to comprise two doublets of peaks, one for each ^{2}H nucleus. In contrast to the ^{1}H case, the ^{2}H dipolar interaction is small and a quadrupolar splitting occurs due to an interaction between the electric quadrupole moment of the ^{2}H nucleus and the gradient of surrounding electric fields. The quadrupole splitting depends on the direction of the external magnetic field vector $\mathbf{B}_0$ with respect to the axes of the electric field gradient (EFG) tensor. Whereas in the ^{1}H case, it is the orientation of the H–H line that determines the magnitude of dipolar splitting, in the case of ^{2}H the orientation of the O–D bond becomes important instead, since in the D_2O molecule the principal axis of the EFG tensor at the hydrogen site points approximately along the O–D bond. This is an essential difference between the NMR interactions in H_2O and D_2O that allows for extracting more complete information about the orientation of water molecule in the beryl voids: The isotopes ^{1}H and ^{2}H serve as two completely different probes. Since the values of dipolar splitting in ^{1}H and quadrupole splitting in the ^{2}H NMR spectra depend significantly on the orientations of water molecules, we can evaluate the orientation and dynamics of the water molecules by analyzing the

temperature dependences of the measured dipolar and quadrupolar splittings.

II. METHODS

Four high-quality synthetic beryl single crystals were studied: two samples containing normal water and two containing heavy water. The samples were grown from oxides on seed plates at 600 °C and 1.5 kbar in a hermetically sealed gold vessel by the hydrothermal method of Thomas and Klyakhin.[16] All samples were cut into cylinders about 2 mm in diameter, with one sample for each hydrogen isotope having the hexagonal axis oriented parallel to the axis of cylinder and the other perpendicular to it. All beryl samples contained type-I water predominately; because of the artificial origin of the samples, the content of alkali atoms and other such impurities and, hence, also the content of type-II water were negligible.

NMR spectra of water-containing beryl single crystals were acquired in a magnetic field of 9.41 T (Larmor frequency $f_0 = 400.185$ MHz for ^{1}H and 61.431 MHz for ^{2}H) using a Bruker Avance II spectrometer. Solid echo pulse sequences $90^\circ_x - \tau - 90^\circ_y - \tau$ (with lengths of the 90° pulses 0.5–1.2 μs for ^{1}H and 3.5–5.0 μs for ^{2}H, and with a delay of $\tau \approx 60$ μs) were applied to excite the NMR signal in order to ensure proper refocusing of the spin magnetization in the presence of strong nuclear dipolar interaction (^{1}H case) or electric quadrupole interaction (^{2}H case). In cases with very large quadrupole splittings, the lines were not excited optimally in the whole range, leading to a slight distortion at the edges of the spectrum. The trigger delays between the subsequent scans were adjusted at each temperature point in order to compensate the strong temperature dependence of the spin-lattice relaxation time. Its value amounted to about 1 and 20 s for ^{1}H and ^{2}H, respectively, at the highest temperatures and to more than 100 s for both isotopes at the lowest temperatures. At each temperature point, 2–64 scans (^{1}H spectra) or 8–1024 scans (^{2}H spectra) were performed, and the acquired spin echo signals were coherently summed.

The temperature dependences were measured in a Janis helium continuous flow cryostat, and the temperature was monitored with Cernox CX-1030 temperature sensor in the proximity of the NMR coil. The orientation of the beryl crystal with respect to the external magnetic field was adjusted carefully with an estimated error of less than 3°. Using a goniometer, the angular dependence of ^{2}H spectra was measured at room temperature.

Special care was taken to keep parasitic ^{1}H signals at the minimum level. We used a custom-made NMR probe without any plastic or Teflon parts and an NMR coil made from unvarnished silver wire. The probe and the sample were dehumidified prior to the experiments. The remaining small parasitic ^{1}H signal near Larmor frequency most probably originated from the cap of the temperature sensor.

III. RESULTS

^{1}H and ^{2}H NMR spectra were measured in the temperature range 5–360 K, and for each isotope two cylindrical samples were studied: In one, the hexagonal crystallographic axis was parallel to the cylinder axis and in the other perpendicular to it. We first describe and interpret the room temperature spectra of ^{1}H and ^{2}H, then we deal with their temperature dependences in the range of approximately 5–360 K.

A. ^{1}H NMR spectra at room temperature

The room temperature ^{1}H NMR spectrum of water molecules in beryl [Fig. 2(a)] consists of a doublet of peaks, originating in the magnetic dipolar interaction between the two ^{1}H nuclei in the water molecule. The value of the dipolar splitting Δ_D depends on the dipolar constant δ as well as on the orientation of the line connecting the interacting nuclei with respect to the direction of the external magnetic field $\mathbf{B}_0$, which is described by a polar angle ϑ_D,[12]

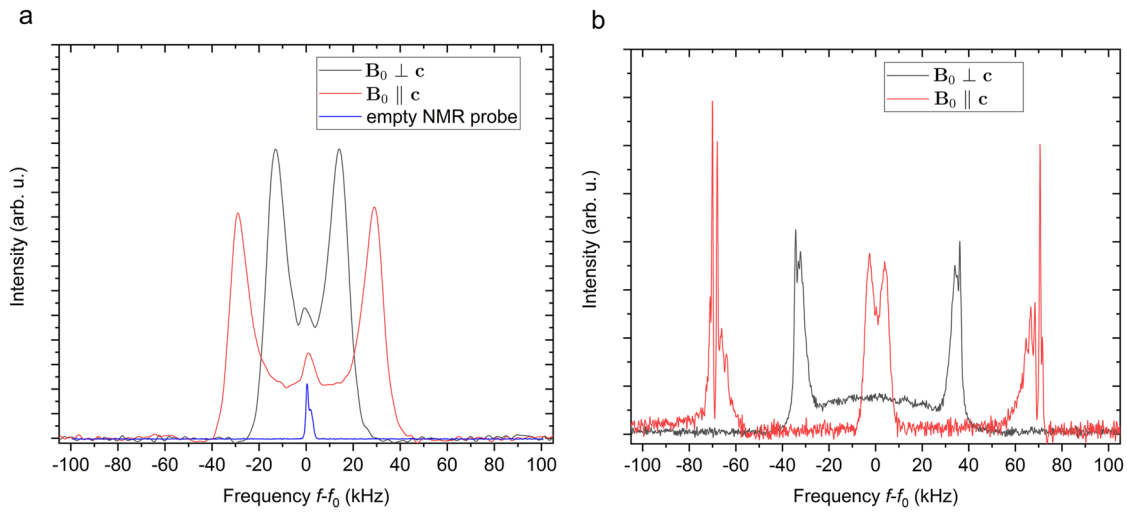

FIG. 2. ^{1}H (a) and ^{2}H (b) NMR spectra of water in beryl measured at room temperature under two experimental settings, with the external magnetic field $\mathbf{B}_0$ oriented perpendicular and parallel with respect to the hexagonal axis **c** of the crystal, respectively. Near $f = f_0$, the ^{1}H spectra contain a small parasitic signal originating from the NMR probe.

$$\Delta_D = \delta\left(3\cos^2\vartheta_D - 1\right), \quad \delta = \frac{3}{2}\frac{\mu_0}{4\pi}\frac{\gamma^2\hbar}{r^3}. \tag{1}$$

The dipolar constant δ depends on the gyromagnetic ratio γ of the interacting nuclei, and it decays with the third power of their mutual distance r. Clearly, the dipolar splitting Δ_D in the measured spectra is different for the two displayed orientations of the crystal with respect to the external magnetic field as the parallel orientation ($\mathbf{B}_0 \| \mathbf{c}$) corresponds to $\vartheta_D \approx 0°$ and the perpendicular one ($\mathbf{B}_0 \perp \mathbf{c}$) to $\vartheta_D \approx 90°$. The larger splitting observed for the parallel orientation implies that the lines connecting the hydrogen atoms (H–H) in the water molecules are preferentially oriented nearly along the hexagonal axis of beryl crystal, i.e., type-I water is observed in the ^{1}H NMR spectra. No signals corresponding to type-II water sites were detected, which is in accord with the supposed negligible concentration of alkali metal atoms in the studied synthetic beryl crystals.

The room temperature values of the observed dipolar splitting $\Delta_D \approx 59$ kHz and $\approx$29 kHz for the parallel and perpendicular orientations, respectively, are significantly smaller than expected for a dipolar interaction between two ^{1}H nuclei in a type-I oriented water molecules. In fact, the dipolar constant δ between two ^{1}H nuclei is given [see Eq. (1)] by their distance r, which is relatively well known ($r \approx 1.524$ Å). An orientation with the H–H line parallel ($\vartheta_D = 0°$) or perpendicular ($\vartheta_D = 90°$) to the external field would therefore yield a splitting of the doublet $\Delta_D = 117$ and 58.7 kHz, respectively. Such discrepancy can be explained by (i) the actual value of the angle ϑ_D being appreciably different from 0 or 90° or by (ii) an averaging of the dipolar interaction strength due to rapid molecular motions. Later in the text (Sec. IV), we show that both mechanisms are responsible for the reduction of the observed dipolar splitting.

Additionally, the ^{1}H nuclei in the water molecules are affected by dipolar interactions with other nuclear species in the surroundings, mainly the ^{1}H nuclei of other water molecules in the neighboring voids and ^{27}Al nuclei in the beryl crystal structure. However, these distant partners induce much weaker dipolar fields, and thus these interactions only lead to a broadening of the resonance peaks. Moreover, despite our efforts to avoid any hydrogen-containing materials in the vicinity of the radio frequency coil, a small parasitic ^{1}H line was detected close to the Larmor frequency. This originated probably from hydrogen atoms present in a small amount in the body of the NMR probe or in the coating of the Cernox temperature sensor.

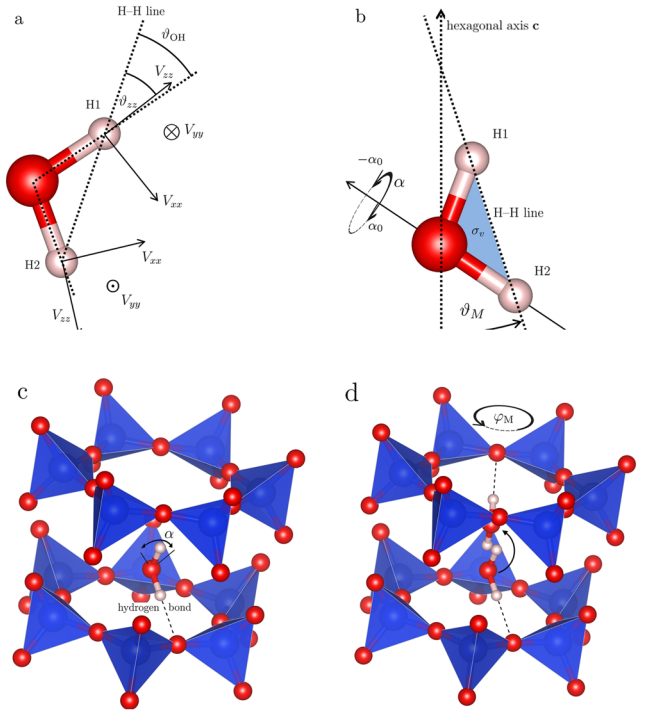

FIG. 3. (a) The principal axis system of the EFG tensor at the hydrogen sites of the water molecule. Definition of the angles ϑ_{zz} and ϑ_{OH} is shown. (b) Orientation of the water molecule with respect to the hexagonal axis. The angle ϑ_M defines the deviation of the H–H line from the hexagonal axis, the angle α describes librations around the axis O–H2 within range $\alpha \in (-\alpha_0, \alpha_0)$. (c) Proposed librational movement of the water molecule in the beryl void. The axis of libration (defined by the O–H2 bond) is aligned with the hydrogen bond formed between the H2 and one of the 12 oxygen atoms in the walls. (d) Proposed molecular jumps among different bonding sites in the void lead to effective rotations around the hexagonal axis (angle φ_M).

B. ^{2}H NMR spectra at room temperature

The ^{2}H NMR spectrum of beryl containing deuterated water is more complex. When the hexagonal axis of beryl crystal is oriented parallel to the external magnetic field, a pair of well-resolved doublets is observed in the ^{2}H spectrum: an outer doublet with a larger splitting of ≈140 kHz and an inner doublet with a splitting of ≈7 kHz. In contrast to the ^{1}H case, these doublets are formed as a result of the electric quadrupole interaction at each ^{2}H nucleus. The presence of two distinct quadrupole doublets in the spectrum implies that the two ^{2}H nuclei in the water molecules are nonequivalent. This in

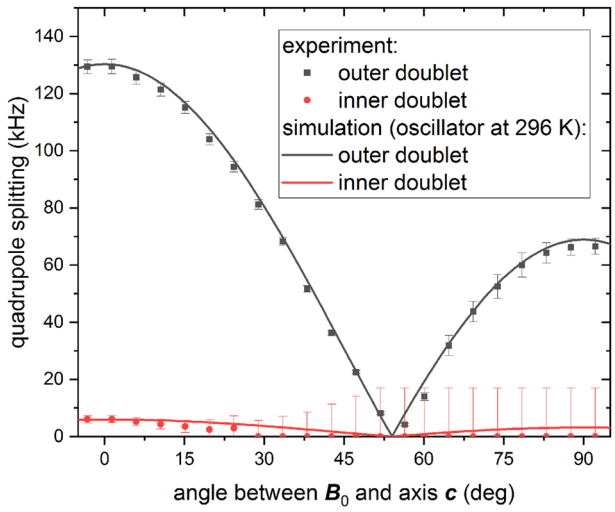

FIG. 4. Temperature dependences of ^{1}H and ^{2}H NMR spectra of water in beryl single crystals. On top, ^{1}H spectra were recorded with the hexagonal axis of beryl sample oriented parallel (a) and perpendicular (b) with respect to the external magnetic field, respectively. Analogous configuration was used for ^{2}H spectra displayed in the bottom (c) and (d).

turn implies that the mean orientation of the H–H line (averaged by rapid molecular motions) of individual water molecules does not point along the hexagonal axis.

Similar to the dipolar splitting in the ^{1}H case, the electric quadrupole splitting Δ_Q also depends on the orientation of the water molecules with respect to the external magnetic field, yet in a more complex way as follows:[12,17]

$$\Delta_Q = \frac{3}{4} C_Q \left(3\cos^2\vartheta_Q - 1 + \eta \sin^2\vartheta_Q \cos 2\varphi_Q\right), \quad (2)$$

$$C_Q = \frac{eQV_{zz}}{h}. \quad (3)$$

The polar ϑ_Q and azimuthal φ_Q angles characterize the direction of the external magnetic field $\mathbf{B}_0$ within the principal axis system (PAS) of the EFG tensor V, which is described by two parameters: the largest component V_{zz}, $|V_{zz}| \geq |V_{yy}| \geq |V_{xx}|$, and a dimensionless asymmetry factor $\eta = \frac{V_{xx} - V_{yy}}{V_{zz}}$, $0 \leq \eta \leq 1$. For the hydrogen site in the water molecule, the principal axis belonging to V_{zz} of the tensor V points approximately along the O–D bond and V_{yy} is perpendicular to the D_2O molecular plane [Fig. 3(a)]. The electric quadrupole interaction constant C_Q is given by the nuclear quadrupole moment of ^{2}H, $Q = 2.85783(30)$ mb (milibarn, 1 mb = 10^{-31} m^2),[18] and by the value of V_{zz} at the ^{2}H nucleus, which depends significantly on the phase of water. In the gas phase, $C_Q = 307.5(6)$ kHz with $\eta = 0.138(1)$,[19,20] in liquid water $C_Q = 250(7)$ kHz[21,22] (η is not known in liquid, but its value is estimated to be similar to those in other phases), and $C_Q = 213.4(3)$ kHz with $\eta = 0.112(5)$ in ice I_h.[23] The values of C_Q for ^{2}H in liquid and ice are reduced compared to the gas phase due to numerous interactions with neighboring molecules via hydrogen bonds in the condensed phases. The quadrupole constant C_Q of ^{2}H in heavy water confined within the beryl voids is unknown, but its value can be expected roughly around 200–300 kHz. The magnitude of the observed quadrupole splitting at room temperature [Fig. 2(b)] is again diminished due to molecular motions, similarly as in the case of ^{1}H dipolar splitting in H_2O.

The dipolar interaction within the water molecule, which is the dominating interaction in the ^{1}H spectra, is much weaker in the case of ^{2}H due to the magnetic moment of the ^{2}H nucleus being 6.5× smaller than the moment of ^{1}H. The intramolecular ^{2}H–^{2}H dipolar interactions thus manifest only as a fine splitting (≈2 kHz) of the spectral lines, which is well noticeable for the peaks of the outer quadrupole doublet [see Fig. 2(b)], and any further dipolar interaction may be neglected.

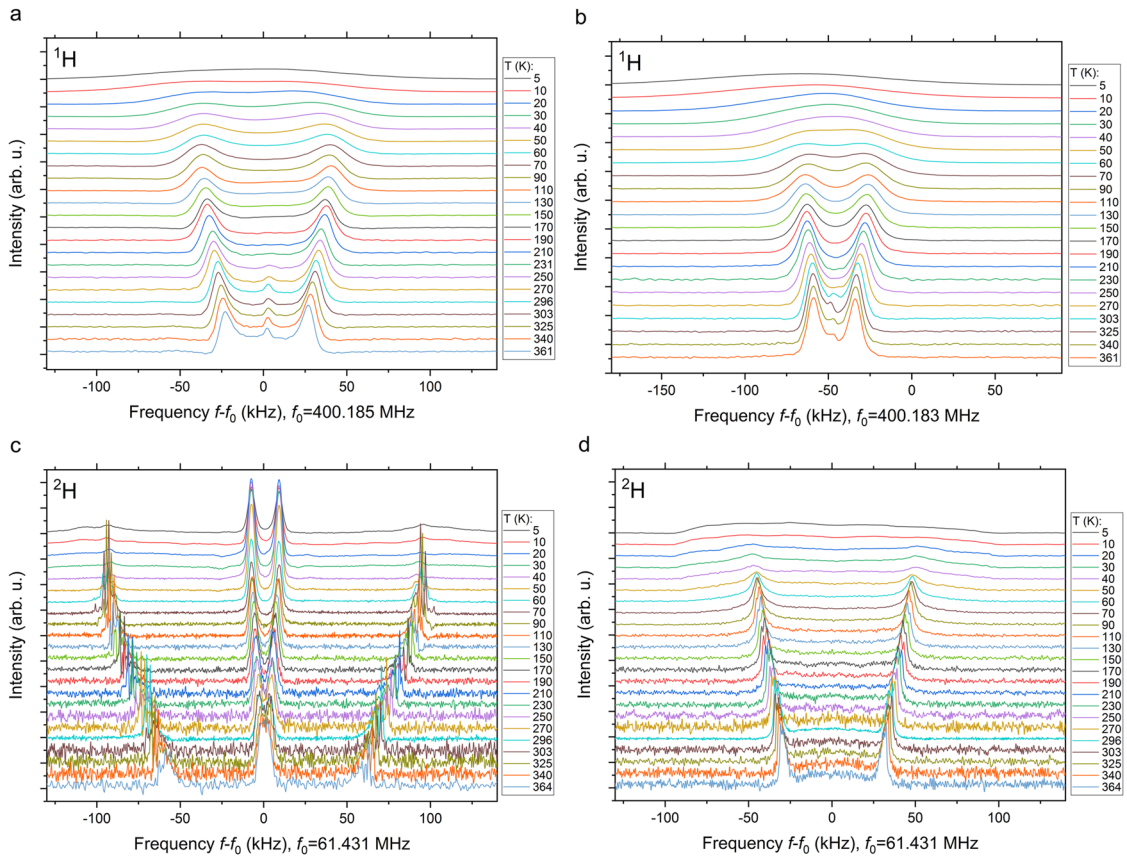

FIG. 5. Angular dependences of the quadrupole splittings Δ_Q obtained from the ^{2}H NMR spectra of a deuterated beryl single crystal at room temperature. Symbols denote experimental data points, solid lines represent dependence simulated using linear harmonic oscillator model described in Sec. IV.

In the $\mathbf{B}_0 \perp \mathbf{c}$ orientation [Fig. 2(b)], the ^{2}H NMR spectrum also consists of two doublets; however, only the outer one is well resolved. The peaks of the inner doublet with a smaller splitting overlap and they are severely broadened, especially at lower temperatures. This behavior can be well observed in the angular dependence of the ^{2}H quadrupole splitting Δ_Q measured for several angles between the two extreme cases $\mathbf{B}_0 \perp \mathbf{c}$ and $\mathbf{B}_0 \parallel \mathbf{c}$ (Fig. 4). The peaks of the inner doublet are resolved only for angles between $\mathbf{B}_0$ and $\mathbf{c}$ below 30°. The excessive broadening is caused by insufficient motional averaging with respect to the hexagonal axis as we explained below in Sec. IV.

C. Temperature dependence of ^{1}H and ^{2}H NMR spectra

The temperature dependent ^{1}H and ^{2}H NMR spectra within 5–364 K are displayed in Fig. 5. The dipolar and quadrupole splittings Δ_D, Δ_Q increase upon cooling, and they level off at about 70 K, which is well seen in the temperature dependence of splittings in Fig. 6. The magnitude of the observed ^{1}H dipolar splitting and its temperature behavior are in agreement with ^{1}H NMR data available in the literature,[14,15] where this behavior was explained by oscillations of the water molecules around their equilibrium positions along the hexagonal axis. This interpretation, however, conflicts with the fact that the dipolar splittings do not reach the expected values even at the lowest temperatures. This leads us unambiguously to the conclusion that the motions of the water molecules have to be more complex than this. As for the ^{2}H spectra, we are aware of no published measurements of the quadrupole splitting of ^{2}H of D_2O in beryl crystal. Our experiments reveal that the ^{2}H spectra follow qualitatively the same pattern as the ^{1}H ones—the splittings of the quadrupole doublets decrease upon cooling in a similar manner.

Below 70 K, the ^{1}H and ^{2}H spectral peaks become significantly broader, indicating a slowing down of the molecular motions so that the averaging of the anisotropic interactions (magnetic dipolar for ^{1}H and electric quadrupole for ^{2}H) becomes inefficient. Thus, at the lowest temperatures, the spectral shapes resemble features typical of static NMR spectra of randomly oriented powder samples. The temperature dependences of the measured NMR spectra and their spectral shapes are analyzed in more detail below.

IV. ANALYSIS AND DISCUSSION

In this section, we show that the established notion of the behavior of water molecules in beryl, i.e., motions with equilibrium positions along the hexagonal axis, is not consistent with the measured NMR data. Furthermore, we propose a new type of movement when the water molecule is bonded via a hydrogen bond to an oxygen atom in the enclosing wall of the beryl void. A detailed analysis allows us to explain all the features observed in the NMR experiment.

The key to determining the motions of the water molecule in beryl lies in a fundamental difference between the ^{1}H and ^{2}H NMR spectra. The dipolar splitting of ^{1}H peaks depends on the orientation of the ^{1}H–^{1}H line with respect to the direction of external magnetic field [via the angle ϑ_D in Eq. (1)]. In contrast, the quadrupole splitting of ^{2}H peaks depends on the direction of the external magnetic field within the PAS of the EFG tensor [via the angles ϑ_Q and φ_Q in Eq. (3)]. The hydrogen atoms in the water molecule are (chemically) equivalent, and, therefore, the ^{2}H EFG tensors are of the same magnitude. However, the orientation of the PAS differs for the two ^{2}H positions in the water molecule since for both EFG tensors the principal axis V_{zz} points approximately along the respective O–H bond, and the water molecule is not linear [Fig. 3(a)]. As a consequence, the angles ϑ_Q and φ_Q are in general different for the two ^{2}H sites.

A. Model for motion of water molecules in beryl voids

For the sake of spectral analysis, let us provisionally assume that the type-I water molecules perform the traditionally accepted type of motion within the void of the beryl crystal as follows: Let the equilibrium orientation of the molecules be such that the H–H line is aligned with the hexagonal axis **c** of the beryl structure, and the molecules may rotate and oscillate around the H–H line within a limited spatial angle around axis **c**—as dictated by the shape and dimensions of the void. Owing to such a motion, the angle ϑ_D is averaged to zero for the case when the external field $\mathbf{B}_0 \parallel \mathbf{c}$, or to 90° for $\mathbf{B}_0 \perp \mathbf{c}$, and a qualitative agreement is reached with the temperature dependences of ^{1}H NMR (Fig. 5) and with ^{1}H NMR data in previous studies.[14,15] However, the observed dipolar splittings Δ_D are somewhat lower than expected based on the distance of ^{1}H nuclei in the water molecule, suggesting that the angle ϑ_D is on average different from 0 or 90°. An even more convincing argument against the considered type of motion is revealed by ^{2}H NMR where two distinct quadrupole doublets are observed in the spectra for $\mathbf{B}_0 \parallel \mathbf{c}$ [Fig. 2(b)]. The D–D line has the same orientation with respect to PAS of EFG of both deuterium sites (due to symmetry of the water molecule). Therefore, rapid rotations or similar molecular motions about the D–D line aligned along the hexagonal axis would yield the same average angle ϑ_Q for both ^{2}H nuclei, and hence the observed quadrupole splitting of ^{2}H would be the same. However, it is clear from the measured ^{2}H NMR spectra that the quadrupole splitting, and thus also the averaged angle ϑ_Q is significantly different for each of the two sites of deuterium in the water molecule.

In principle, the large quadrupole splitting of the outer doublet in the ^{2}H spectrum could be compatible with a situation where the D–D line lies approximately along the hexagonal axis, but the splitting of the second, inner doublet would not comply. The quadrupole splitting of the inner doublets is so small that it can only be reached if the magnetic field maintains a very specific orientation with respect to the PAS of EFG of such a ^{2}H atom: The angle ϑ_Q must be (on average) close to the value 54.7°, so called "magic angle" for which the expression $3\cos^2\vartheta_Q - 1$ in Eq. (3) becomes zero. This condition can be satisfied when the D–D line of the water molecule is deviated from the beryl hexagonal axis by an angle $\vartheta_M \approx 19.5°$ [Fig. 3(b)]. The principal axis V_{zz} at the deuterium site is slightly deviated from the direction of the O–D bond of the water molecule by about 1.35°.[20] If we assume the H–O–H angle to equal 106.9°,[3,24] the angle ϑ_{OH} between the O–H bond and the H–H line equals 36.55° (see Fig. 3). Using the same geometry for D_2O, these values yield the value of angle ϑ_{zz} of 35.2°. Then, $\vartheta_Q = \vartheta_{zz} \pm \vartheta_M$ gives values of $\vartheta_Q = 54.7°$ and 15.7°, the first one being close to the magic angle.

For the deduced value of angle $\vartheta_M \approx 19.5°$, the O–D bond may conveniently point toward any of the enclosing oxygen atoms,

which forms a suitable arrangement for creation of hydrogen bond [Fig. 3(c)]. Therefore, the reason for such peculiar arrangement of the water molecules is apparently the formation of a hydrogen bond between the deuterium atom in D_2O and one of the oxygen atoms that form the walls of the beryl voids. Therefore, we propose a model in which the water molecules attach to an oxygen atom via a hydrogen bond, and the molecules perform two distinct motions: First, they librate rapidly about the formed hydrogen bond [Fig. 3(c)]. Since hydrogen bonds tend to be highly directional,[25] the axes of libration coincide with the O–H bonds of the molecules and these axes deviate from the beryl hexagonal axis **c** by an angle close to the magic angle 54.7°. Second, since the water molecules may form the hydrogen bonds with any of the 12 oxygen atoms available in the walls of the voids, the molecules are also expected to jump among these available bonding sites [Fig. 3(d)], i.e., they effectively rotate about the beryl hexagonal axis. In the following analysis, we show that these two types of motion can explain the NMR experiment even quantitatively.

Naturally, the jumps accompanied by re-bonding of hydrogen bond have to be slower than the librations about the O–H bond, yet both these molecular motions are fast enough to cause averaging effects in NMR. The frequency shifts or splittings in the NMR spectra are usually orders of magnitude smaller compared to the rate of change of local fields induced by such molecular motions. As a consequence, the measured ^{1}H and ^{2}H NMR spectra of water in beryl are affected by averaged dipolar and quadrupole interactions, which is documented by the reduced values of splittings and by the presence of narrow spectral peaks at higher temperatures. Upon lowering the temperature, the frequencies and amplitudes of molecular motions decrease, therefore the splittings approach their nominal values, and the spectral peaks broaden.

B. Analysis of librations of water molecules

In order to analyze the first mode of molecular motion (i.e., the rapid librations of the molecule about the hydrogen bond), we denote by ϑ_M the angle describing the deviation of the H–H line from the hexagonal axis of the beryl crystal [Fig. 3(b)]. The librations of the molecule about its axis O–H2 are described by the angle α, which is zero for the apex position (i.e., when the hexagonal axis **c** is parallel to the mirror plane σ_v, which contains all three atoms of the water molecule), and we suppose it librates around the mean position with an amplitude of α_0, $\alpha \in (-\alpha_0, \alpha_0)$. For now, we assume the angle α to be distributed uniformly within its limits $(-\alpha_0, \alpha_0)$, which enables us to express the average dipolar and quadrupole splittings as

$$\langle \Delta_D \rangle_{OH} = \frac{1}{2\alpha_0} \int_{-\alpha_0}^{\alpha_0} \Delta_D \, d\alpha,$$
$$\langle \Delta_Q \rangle_{OH} = \frac{1}{2\alpha_0} \int_{-\alpha_0}^{\alpha_0} \Delta_Q \, d\alpha. \tag{4}$$

The second type of motion is connected with re-bonding of the H2 atom to any of the remaining five oxygen sites or, instead, with H1 atom forming a hydrogen bond with one of the six oxygen sites in the other hemisphere [Fig. 3(d)]. Such jumps cause averaging with respect to the hexagonal axis **c** of beryl, which we can consider as rotational averaging over the angle φ_M in the full $\langle 0, 2\pi)$ range. The dipolar and quadrupole splittings, averaged by both types of movements, can then be expressed as functions of the angles ϑ_{OH}, ϑ_{zz}, ϑ_M, and α_0 as follows:

$$\langle\langle \Delta_D \rangle\rangle_{OH,c} = \frac{1}{2\pi} \frac{1}{2\alpha_0} \int_0^{2\pi} \int_{-\alpha_0}^{\alpha_0} \Delta_D \, d\alpha \, d\varphi_M,$$
$$\langle\langle \Delta_Q \rangle\rangle_{OH,c} = \frac{1}{2\pi} \frac{1}{2\alpha_0} \int_0^{2\pi} \int_{-\alpha_0}^{\alpha_0} \Delta_Q \, d\alpha \, d\varphi_M. \tag{5}$$

The averaged splittings $\langle\langle \Delta_D \rangle\rangle_{OH,c}$ and $\langle\langle \Delta_Q \rangle\rangle_{OH,c}$ further depend also on the dipolar constant δ and the quadrupolar parameters C_Q and η, respectively. The value of δ is given by the distance between the ^{1}H nuclei [Eq. (1)] and thus it is closely linked to the geometry of the water molecule. C_Q and η are unknown for water confined in beryl but they should not be dramatically different from the values for D_2O in various phases, i.e., $C_Q \approx 200 - 300$ kHz and $\eta \approx 0.1$. Moreover, the angles ϑ_{OH} and ϑ_{zz} are given by the geometry of water molecule [Fig. 3(a)]. In further analysis, we assume the value of the H–O–H angle of 106.9° and a H–O distance of 0.949 Å, which was found by neutron diffraction experiments.[3,24] These parameters yield a value of $\vartheta_{OH} = 36.55°$ for the angle between the H–H line and the O–H bond. The angle ϑ_{zz} between the H–H line and the principal axis V_{zz} is then equal to 35.2°, which corresponds to a small deviation (≈1.35°) of the V_{zz} axis from the direction of the O–H bond as determined from hyperfine structure measurements of heavy water.[20] The H–H distance is equal to 1.525 Å and thus $\delta \approx 58.7$ kHz, according to Eq. (1). Based on these values, the remaining parameters of interest, angles ϑ_M and α_0, can be determined from our NMR experiments using a suitable model.

The angle ϑ_M determines the deviation of the libration axis O–H from the hexagonal axis and its value dictates, to a great extent, the specific character of the observed ^{2}H spectra, i.e., the positions of the two doublets with distinctly different quadrupole splittings. Whereas the dipolar splitting in ^{1}H spectra as well as the quadrupole splitting of outer doublets in ^{2}H spectra do not vary much with deviation of the axis of libration (angle ϑ_M), the small quadrupole splitting of the inner doublet in the ^{2}H spectra is particularly sensitive to the changes in the ϑ_M angle [Fig. 7(a)]. For both sample orientations $\mathbf{B}_0 \perp \mathbf{c}$ and $\mathbf{B}_0 \parallel \mathbf{c}$, the splitting of the inner doublet becomes zero when $\vartheta_Q = \vartheta_{zz} + \vartheta_M$ reaches the magic angle. One may notice that there are two possible values of ϑ_M that yield the small splitting of the inner doublets observed in experiment; this issue will be addressed in further analysis below.

The peaks of the inner doublet in the ^{2}H spectrum become substantially broadened for $\mathbf{B}_0 \perp \mathbf{c}$ (as well as for any orientations where the external magnetic field $\mathbf{B}_0$ is deviated from the hexagonal axis **c** by more than ≈30°, see Fig. 4), and this broadening becomes even more pronounced with decreasing temperature. For $\mathbf{B}_0 \perp \mathbf{c}$, the splitting of the inner doublet depends strongly on the angle φ_M [Fig. 7(b)]. Consequently, for the inner doublet, averaging over the angle φ_M becomes ineffective already at temperatures below room temperature, whereas the averaging is still effective enough for the outer doublet to be well resolved. The averaging of $\langle\langle \Delta_D \rangle\rangle_{OH,c}$ and $\langle\langle \Delta_Q \rangle\rangle_{OH,c}$ in Eq. (5) is assumed to be continuous in angle φ_M, whereas in reality there are 12 discrete orientations in the single crystal, i.e., the angle φ_M should take values $\frac{\pi}{6}k + \varphi_{M,0}$, where $k \in \langle 0, 12)$

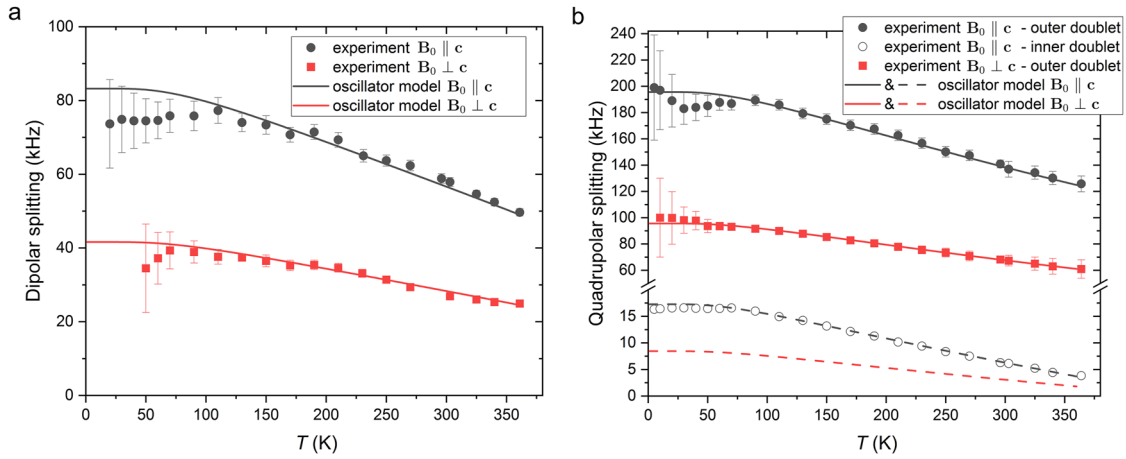

FIG. 6. Comparison of dipolar (a) and quadrupole (b) splittings measured as a function of temperature with those obtained by the model based on harmonic oscillator.

is an integer. However, neither this simplification nor the indeterminacy of the phase angle $\varphi_{M,0}$ leads to any noticeable difference in the averaged values of the splittings.

Although both ϑ_M and α_0 are expected to be temperature dependent, mainly the amplitude of librations α_0 is responsible for the decrease in dipolar and quadrupole splittings with temperature due to motional averaging. The averaged splittings $\langle\langle\Delta_D\rangle\rangle_{OH,c}$ and $\langle\langle\Delta_Q\rangle\rangle_{OH,c}$ as functions of amplitude α_0 are displayed in Fig. 8; the gray areas denote the ranges of amplitudes corresponding to experimentally observed dipolar and quadrupole splittings. The splittings obtained by NMR experiments can thus be related to variations of the amplitude α_0 within the given range. However, even if the calculated dependences roughly capture the range and basic character of experimental splittings (lower values of α_0 correspond to low temperatures and highest α_0 to $T \approx 360$ K), it is clear that there are systematic differences. First, the experimentally detected low-temperature plateaus are not present in the simulated dependences. Second, in the experiment the splitting of the inner quadrupole doublet decays faster with increasing temperature than the splitting of outer doublet—the ratio of splittings for these doublets gradually increases from 11.5 at low temperatures to more than 30 at high temperatures (Fig. 6).

Both these shortcomings can be removed by implementing a specific temperature dependence to angles ϑ_M and α_0. Such dependence, however, may be realized in many different ways, leading to similar levels of agreement with the experiment. We show that a good agreement (Fig. 6) is reached already with probably the simplest approach when the librational motion of the water molecule about one of its O–H axes is considered as that of a quantum harmonic oscillator.

A quantum harmonic oscillator provides quantized energies given by

$$E_n = \hbar\omega\left(n + \frac{1}{2}\right), \tag{6}$$

where ω denotes the angular frequency of the librational motions of the water molecule about the O–H bond. The states with energies E_n are populated with Boltzmann probabilities

$$p_n = \frac{e^{-\frac{E_n}{k_B T}}}{\sum_{n=0}^{\infty} e^{-\frac{E_n}{k_B T}}}, \tag{7}$$

the mean energy can be written as

$$\langle E\rangle = \frac{\sum_{n=0}^{\infty} E_n e^{-\frac{E_n}{k_B T}}}{\sum_{n=0}^{\infty} e^{-\frac{E_n}{k_B T}}} \tag{8}$$

and it is related to the amplitude α_0' as

$$\langle E\rangle = \frac{1}{2} k d_{OH}^2 \langle \sin^2 \alpha_0' \rangle, \tag{9}$$

where d_{OH} is the length of the O–H bond. The force constant k of the oscillator is related to the frequency ω as $k = m\omega^2$, where m is the mass of proton or deuteron for the H_2O or D_2O case, respectively. The value of ω is a free parameter in the harmonic oscillator model, and it accounts for the overall shape of the temperature dependences, with $\omega = \omega_H$ for H_2O and $\omega = \omega_H$ for D_2O. Equations (4) and (5), which assumed a uniformly distributed angle α, now have to be modified because for a Boltzmann-averaged harmonic oscillator the angle α is not distributed uniformly; instead, it has a Gaussian distribution[26] with a dispersion $\alpha_0'^2$. In our case, only a few lowest energy levels of the oscillator are populated even at the highest temperature $T = 365$ K; therefore, the zero-point energy is considerable and a visible plateau up to about 50 K appears in all simulated dependences (Fig. 6).

The fact that upon heating, the splitting of the inner quadrupole doublet decays faster than that of the outer doublet can be captured by making the angle ϑ_M temperature dependent. By increasing ϑ_M slightly with increasing temperature, the value of $\vartheta_Q = \vartheta_{zz} + \vartheta_M$ further approaches the magic angle, which reduces the splittings of the inner quadrupole doublets while leaving the splittings of the outer doublets relatively unchanged [see Fig. 7(a)]. If we thus increase ϑ_M within the range of 18.1–19.2° linearly with temperature in range 5–365 K, the ratio of simulated splittings follows very well the values observed in our experiment (Fig. 6).

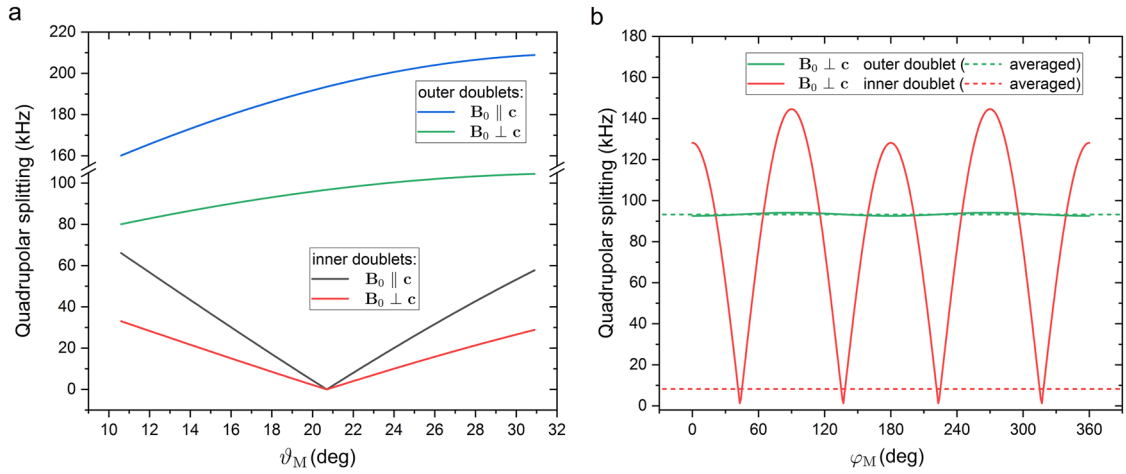

FIG. 7. (a) Dependence of the quadrupole splittings $\langle\langle\Delta_Q\rangle\rangle_{OH,c}$ of doublets in ^{2}H spectra on the tilt angle ϑ_M. The splittings were averaged by librations around O–H bond (amplitude $\alpha_0 = 40°$) and jumps around hexagonal axis (averaging with respect to the angle φ_M). (b) Sensitivity of the quadrupole splittings $\langle\Delta_Q\rangle_c$ to the angle φ_M in case of perpendicular orientation of the magnetic field, angle $\vartheta_M = 18.1°$, and averaging only by the librations ($\alpha_0 = 40°$). Dashed lines correspond to values when the splittings were additionally averaged with respect to the angle φ_M.

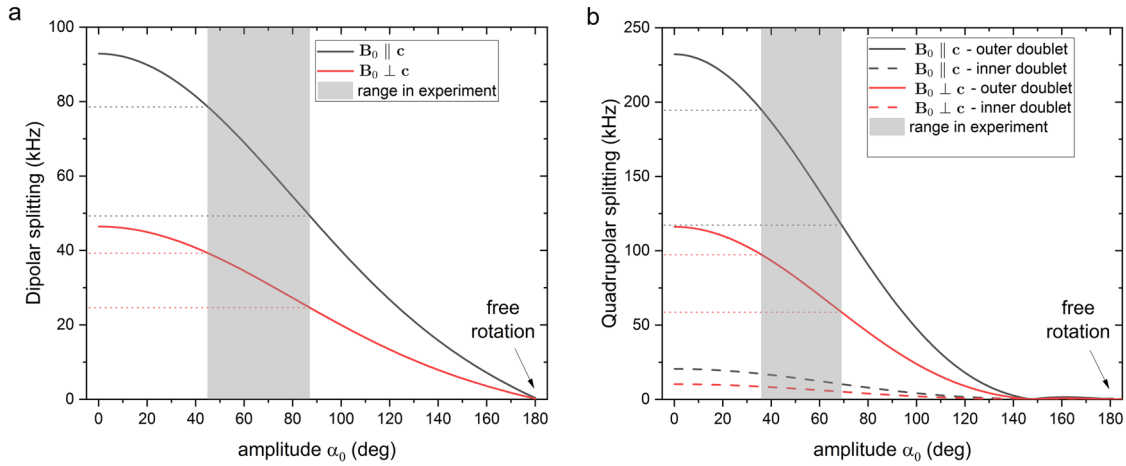

FIG. 8. Calculated averaged dipolar (a) and quadrupole (b) splitting as a function of the angular amplitude of librations α_0. The water molecule is assumed to rotate uniformly within an angular interval $(-\alpha_0, \alpha_0)$ about its O–H2 axis tilted by $\vartheta_M \approx 18.1°$. Additionally, the molecule jumps between different bonding sites (averaging with respect to angle φ_M). Gray areas denote the range of observed values α_0.

In the dependence of quadrupole splittings on angle ϑ_M [Fig. 7(a)], there are apparently two values of $\vartheta_M \approx 18°$ and $\approx 23°$, bringing ϑ_Q close to the magic angle and thus leading to the small splittings of inner doublets in the experiment. The larger value of ϑ_M can also lead to a good agreement of the model with experimental quadrupole splittings, using a different frequency ω, similar quadrupole parameters C_Q and η, and a gradual decrease in ϑ_M with increasing temperature—again to approach the magic angle for ϑ_Q, but this time from above. To discriminate between these two solutions, we can use the dipolar splittings in ^{1}H spectra, where this somewhat larger tilt angle $\vartheta_M \approx 23°$ does not yield a reasonable agreement. In order to match the experiment, we have to use $\delta \approx 69.1$ kHz corresponding to a H–H distance of 1.444 Å, which would lead to an unrealistic H–O–H angle of 99.1° (for an O–H bond-length of 0.949 Å). Moreover, a decrease in the tilt angle ϑ_M with increasing temperature would be required, which lacks a suitable justification. In contrast, for the $\vartheta_M \approx 18°$ solution, an increase in ϑ_M with temperature makes more physical sense: With increasing ϑ_M, the hydrogen H1 points more toward the hexagonal axis **c** (Fig. 3), which provides more space for the oscillating part of the molecule—increasing ϑ_M with temperature is thus a plausible consequence of larger oscillations at high temperatures.

The best match with the experiment is reached for ϑ_M linearly changing in the range 18.1–19.2° (from low to high temperatures), with $\frac{\omega_H}{2\pi} \approx 4.95 \cdot 10^{12}$ Hz for H_2O, which corresponds to a frequency of librations of 165 cm^{-1}. As for the temperature

dependence of the quadrupole splitting in D_2O, the best match is reached using $\frac{\omega_D}{2\pi} \approx 4.34 \cdot 10^{12}$ Hz, corresponding to 145 cm^{-1}. Both these wave numbers are in reasonable agreement with values of libration modes of type-I water as observed in optical experiments.[5,10] Out of the remaining parameters, a part of them is determined by the water molecule geometry—δ = 58.7 kHz, d_{OH} = 0.949 Å, and ϑ_{zz} = 35.2°—and the last two parameters do not significantly differ from expectations—C_Q = 176 kHz and η = 0.13.

We note that the ratio of harmonic frequencies $\frac{\omega_H}{\omega_D} \approx 1.14$ does not reach the value $\sqrt{2}$, which is expected from the ratio of deuteron and proton masses. This is most probably caused by the limitation of our simple oscillator model, where the amplitudes of oscillations are relatively large at high temperatures. Only a few lowest energy levels of the oscillator ensemble are populated even at 365 K as indicated by the sum of the first five Boltzmann probabilities $\sum_{n=0}^{4} p_n \approx 0.96$; therefore, the difference between quantum harmonic oscillator model and, e.g., particle-in-box model would not be large. However, the effect of walls of the beryl voids should be addressed, especially at high temperatures, by adding some particle-in-box features, which would lead to a more appropriate model such as oscillator confined in a box.[27]

Another limitation of the applied model is that the frequency of linear harmonic oscillator is constant and only the amplitude of motion decreases with temperature. In reality, however, the frequency of molecular motions and jumps also reduces on cooling, and at some point the motional averaging becomes inefficient. This is noticeable at temperatures below 70 K where the character of NMR spectra changes and some of the well-resolved doublets become broad bands with features resembling spectra of a powder sample—instead of averaged values, the spectra display the actual distributions of the local fields. The narrow peaks with resonance frequencies corresponding to the time-averaged fields are still apparent at 70 K, whereas the NMR spectra at 30 K already contain broad bands (Fig. 9). The low-temperature spectra are broad and featureless, somewhat reducing exploitable information; nevertheless, we briefly check our approach by comparing them with simulated NMR spectra where the motional averaging was fully or partially removed.

Using the spectroscopic and angular parameters obtained from the linear harmonic oscillator model, we constructed the ^{2}H spectrum for $\mathbf{B}_0 \perp \mathbf{c}$ [Fig. 9(a)] as a histogram where the angle α has a Gaussian distribution (with dispersion $\alpha_0'^2$) and the angle φ_M is uniformly distributed within $\langle(0, 2\pi)$, i.e., a fully static spectrum. Additionally, we simulated a spectrum where the jumps/re-bonding ceased, but the averaging due to librational motion is still effective. Apparently, the experimental spectrum at 30 K contains features of both types of simulated spectra. Similar behavior can be seen for $\mathbf{B}_0 \| \mathbf{c}$ [Fig. 9(b)], where the outer doublet is broadened as in a fully static spectrum, yet it contains some residual peaks at about 100 and -100 kHz, which stem from the librational averaging. On the other hand, the inner doublet for $\mathbf{B}_0 \| \mathbf{c}$ remains unchanged by these effects, which is expected, since it originates from the ^{2}H nuclei of the H2 atoms, which have a delta-function-like or very narrow distribution of motions during the librations—as imposed by the directionality of the hydrogen bond. Unlike for higher temperatures, where Δ_D and Δ_Q were averaged by rapid molecular motions, at low temperatures it becomes important that in reality the angle φ_M takes on discrete values. The shapes of simulated spectra become dependent on the phase $\varphi_{M,0}$, however, they do not yield better agreement with the experiment than the simulated spectra in Fig. 9. Probably the arrangement of water molecules at very low temperatures differs from these simple static models and in order to reach better agreement, additional assumptions would have to be considered about the residual dynamics of the system or the fine details of potential represented by the beryl structure. This may also be connected with the character of hydrogen bonding at very low temperatures, where inelastic neutron scattering measurements[28,29] are interpreted so that hydrogen bonding is weakened or not present at all. On the other hand, low-temperature Raman measurements[30,31] were interpreted including weak hydrogen bond between the water molecule and the beryl walls. Our NMR data at low temperatures do not provide unambiguous interpretation in this regard; however,

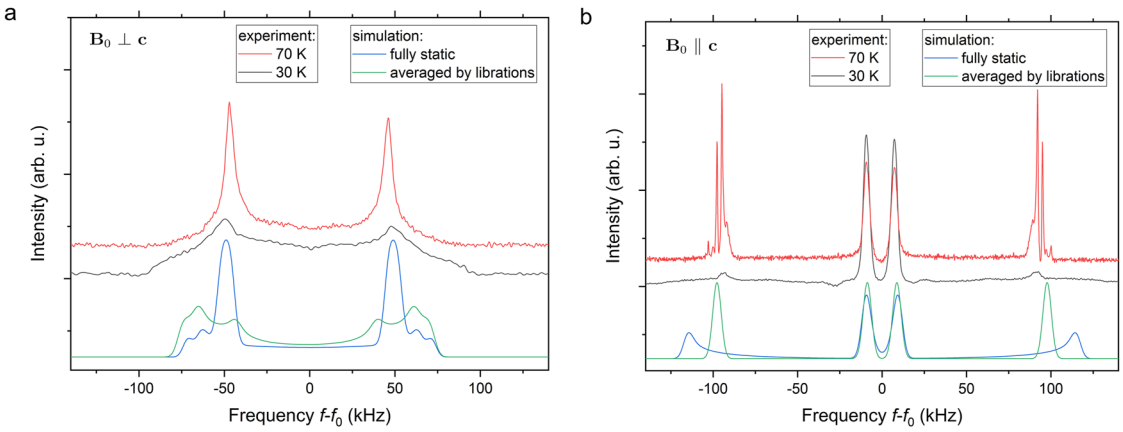

FIG. 9. Experimental ^{2}H NMR spectra of water in beryl at low temperatures for $\mathbf{B}_0 \perp \mathbf{c}$ (a) and $\mathbf{B}_0 \| \mathbf{c}$ (b). Simulated NMR spectra with powder-like features were constructed by removing the molecular jumps (averaging via angle φ_M) or by removing the motions entirely, i.e., considering static, randomly halted molecules.

for temperatures higher than ≈50 K the motional behavior and specific arrangement of water molecules deduced from our experiments clearly suggest the presence of hydrogen bonds.

C. Analysis of jumps and re-bonding of water molecules

The details of the second type of motion of water molecule in the voids—the re-bonding of hydrogen bond leading to effective rotations of the water molecules about the beryl hexagonal axis—are more difficult to obtain from our NMR experiments. The 12 bonding sites in the beryl void are equivalent by symmetry and thus cannot be distinguished directly in the NMR spectrum. From the dispersion of the quadrupole splitting with angle φ_M in the case of $\mathbf{B}_0 \perp \mathbf{c}$ [Fig. 7(b)], it is apparent that the re-bonding (considered as an instantaneous change in φ_M) leads to variations of the splitting $\langle \Delta_Q \rangle_c$ for the inner doublet that are about two orders of magnitude larger than those of the outer doublet. Therefore, the outer doublet is well resolved in the ^{2}H NMR spectrum, i.e., the librations and re-bonding lead to sufficient averaging of local fields for the oscillating part of the water molecule (H1 site), whereas the inner doublet is severely broadened when $\mathbf{B}_0 \perp \mathbf{c}$, which means that the averaging by re-bonding is ineffective. From this, we may estimate that the jumps within the beryl void are about two orders of magnitude slower than the molecular librations.

V. CONCLUSIONS

The experimentally obtained ^{1}H and ^{2}H NMR spectra, measured at temperatures 5–360 K, provided geometric and dynamic information on the behavior of water molecules in beryl crystal. We showed that although the water molecules in the undoped beryl, traditionally denoted as type-I molecules, are indeed oriented preferentially with their H–H lines along the hexagonal axis of beryl, the actual orientation of the H–H lines is significantly (by about 18°) declined from the hexagonal axis. The reason consists apparently in the fact that the water molecules are oriented by their O–H bond toward one of 12 oxygen atoms forming the walls of the beryl structural voids. These positions are obviously energetically favorable as hydrogen bonds between the H_2O molecules and the void walls can be formed. In order to explain satisfactorily our experimental results, we proposed a model within which the molecules perform two types of movements: (i) librations around the axes of such hydrogen bonds and (ii) less frequent orientational jumps among the 12 possible binding sites in the void. A simple thermodynamical model, with the water molecule considered as a quantum harmonic oscillator, correctly describes the observed experimental data at all temperatures, for both normal and heavy water. The frequencies of the oscillatory motions, evaluated from our thermodynamic model, agree well quantitatively with the frequencies of libration motions observed by optical experiments.[5,10]

The implications of our work can be summarized as follows: First of all, the traditional view of type-I water molecules embedded in the beryl voids has to be corrected; a deviation of their H–H lines from the hexagonal axis with a mean value of about 18° must be accounted for. Consequently, in the search for ferroelectric order in the water subsystem, it appears important to bear in mind that, in principle, two components of spontaneous polarization may exist at low temperatures; a net ferroelectric moment may appear not only in the *ab* crystallographic planes but also along the *c* hexagonal axis. Concerning the interactions between the water molecules and the atoms forming the structural voids in beryl, we have provided a very strong indirect indication that hydrogen bonds are formed between the molecules and any of the 12 closest oxygen atoms. This contradicts the earlier conjecture by Paré and Ducros[14] that no hydrogen bonds between the molecules and the beryl structure forms. Conversely, the presence of these hydrogen bonds supports the recent idea of a coupling mechanism between the water molecules and the beryl crystal lattice, suggested recently by Finkelstein *et al.*,[6] which agrees very well also with the observation of sum and difference frequencies in the infrared spectra.[10] Consequently, our findings, as we believe, can serve as a firm basis for further investigations, including theoretical modeling, of the dynamics of isolated water molecules in beryl, and they can thus also deepen the understanding of mechanisms and interactions favoring the ferroelectric ordering of the water molecules.

ACKNOWLEDGMENTS

This work was supported by the Czech Science Foundation (Project No. 20-1527S) and by the MŠMT project SOLID21 (Project No. CZ.02.1.01/0.0/0.0/16_019/0000760).

AUTHOR DECLARATIONS

Conflict of Interest

The authors have no conflicts to disclose.

Author Contributions

Vojtěch Chlan: Conceptualization (equal); Data curation (equal); Formal analysis (equal); Investigation (equal); Methodology (equal); Validation (equal); Writing – original draft (equal); Writing – review & editing (equal). **Martin Adamec**: Data curation (equal); Investigation (equal); Writing – review & editing (equal). **Helena Štěpánková**: Formal analysis (equal); Funding acquisition (equal); Methodology (equal); Validation (equal); Writing – review & editing (equal). **Victor G. Thomas**: Resources (equal). **Filip Kadlec**: Conceptualization (equal); Funding acquisition (equal); Methodology (equal); Project administration (equal); Resources (equal); Validation (equal); Writing – original draft (equal); Writing – review & editing (equal).

DATA AVAILABILITY

The data that support the findings of this study are available from the corresponding author upon reasonable request.

REFERENCES

[1] B. P. Gorshunov, E. S. Zhukova, V. I. Torgashev, E. A. Motovilova, V. V. Lebedev, A. S. Prokhorov, G. S. Shakurov, R. K. Kremer, V. V. Uskov, E. V. Pestrjakov, V. G. Thomas, D. A. Fursenko, C. Kadlec, F. Kadlec, and M. Dressel, "THz–IR spectroscopy of single H_2O molecules confined in nanocage of beryl crystal lattice," Phase Transitions **87**, 966–972 (2014).

[2]B. P. Gorshunov, V. I. Torgashev, E. S. Zhukova, V. G. Thomas, M. A. Belyanchikov, C. Kadlec, F. Kadlec, M. Savinov, T. Ostapchuk, J. Petzelt, J. Prokleška, P. V. Tomas, E. V. Pestrjakov, D. A. Fursenko, G. S. Shakurov, A. S. Prokhorov, V. S. Gorelik, L. S. Kadyrov, V. V. Uskov, R. K. Kremer, and M. Dressel, "Incipient ferroelectricity of water molecules confined to nano-channels of beryl," Nat. Commun. **7**, 12842 (2016).
[3]A. I. Kolesnikov, G. F. Reiter, N. Choudhury, T. R. Prisk, E. Mamontov, A. Podlesnyak, G. Ehlers, A. G. Seel, D. J. Wesolowski, and L. M. Anovitz, "Quantum tunneling of water in beryl: A new state of the water molecule," Phys. Rev. Lett. **116**, 167802 (2016).
[4]E. S. Zhukova, V. I. Torgashev, B. P. Gorshunov, V. V. Lebedev, G. m. S. Shakurov, R. K. Kremer, E. V. Pestrjakov, V. G. Thomas, D. A. Fursenko, A. S. Prokhorov, and M. Dressel, "Vibrational states of a water molecule in a nano-cavity of beryl crystal lattice," J. Chem. Phys. **140**, 224317 (2014).
[5]M. A. Belyanchikov, E. S. Zhukova, S. Tretiak, A. Zhugayevych, M. Dressel, F. Uhlig, J. Smiatek, M. Fyta, V. G. Thomas, and B. P. Gorshunov, "Vibrational states of nano-confined water molecules in beryl investigated by first-principles calculations and optical experiments," Phys. Chem. Chem. Phys. **19**, 30740–30748 (2017).
[6]Y. Finkelstein, R. Moreh, S. L. Shang, Y. Wang, and Z. K. Liu, "Quantum behavior of water nano-confined in beryl," J. Chem. Phys. **146**, 124307 (2017).
[7]V. Arivazhagan, F. D. Schmitz, P. E. Vullum, A. T. J. van Helvoort, and B. Holst, "Atomic resolution imaging of beryl: An investigation of the nano-channel occupation," J. Microsc. **265**, 245–250 (2017).
[8]G. V. Gibbs, D. W. Breck, and E. P. Meagher, "Structural refinement of hydrous and anhydrous synthetic beryl, $Al_2(Be_3Si_6)O_{18}$ and emerald, $Al_{1.9}Cr_{0.1}(Be_3Si_6)O_{18}$," Lithos **1**, 275–285 (1968).
[9]K. Momma and F. Izumi, "*VESTA* 3 for three-dimensional visualization of crystal, volumetric and morphology data," J. Appl. Crystallogr. **44**, 1272–1276 (2011).
[10]D. L. Wood and K. Nassau, "Infrared spectra of foreign molecules in beryl," J. Chem. Phys. **47**, 2220–2228 (1967).
[11]M. Dressel, E. S. Zhukova, V. G. Thomas, and B. P. Gorshunov, "Quantum electric dipole lattice," J. Infrared, Millimeter, Terahertz Waves **39**, 799–815 (2018).
[12]A. Abragam, *The Principles of Nuclear Magnetism* (Oxford University Press, 1961).
[13]K. Modig and B. Halle, "Proton magnetic shielding tensor in liquid water," J. Am. Chem. Soc. **124**, 12031–12041 (2002).
[14]X. Paré and P. Ducros, "Étude par résonance magnétique nucléaire de l'eau dans le béryl," Bull. Soc. Fr. Minéral. Cristallogr. **87**, 429–433 (1964).
[15]Y. Sugitani, K. Nagashima, and S. Fujiwara, "The NMR analysis of the water of crystallization in beryl," Bull. Chem. Soc. Jpn. **39**, 672–674 (1966).
[16]V. Thomas and V. Klyakhin, "The specific features of beryl doping by chromium under hydrothermal conditions," in *Mineral Forming in Endogenic Processes*, edited by N. Sobolev (Nauka, Novosibirsk, 1987), pp. 60–67 (in Russian).
[17]D. Freude, "Quadrupolar nuclei in solid-state nuclear magnetic resonance," in *Encyclopedia of Analytical Chemistry*, edited by R. Meyers (John Wiley & Sons, Chichester, 2000), pp. 12188–12224.
[18]P. Pyykkö, "Year-2017 nuclear quadrupole moments," Mol. Phys. **116**, 1328–1338 (2018).
[19]R. M. Garvey and F. C. D. Lucia, "Extension of high resolution beam maser spectroscopy into the submillimetre wave region," Can. J. Phys. **55**, 1115–1123 (1977).
[20]H. Bluyssen, J. Verhoeven, and A. Dymanus, "Hyperfine structure of HDO and D_2O by beam maser spectroscopy," Phys. Lett. A **25**, 214–215 (1967).
[21]R. P. W. J. Struis, J. De Bleijser, and J. C. Leyte, "Dynamic behavior and some of the molecular properties of water molecules in pure water and in magnesium chloride solutions," J. Phys. Chem. **91**, 1639–1645 (1987).
[22]B. C. Gordalla and M. D. Zeidler, "Molecular dynamics in the system water-dimethylsulphoxide," Mol. Phys. **59**, 817–828 (1986).
[23]D. T. Edmonds and A. L. Mackay, "The pure quadrupole resonance of the deuteron in ice," J. Magn. Reson. **20**, 515–519 (1975).
[24]G. D. Gatta, F. Nestola, G. D. Bromiley, and S. Mattauch, "The real topological configuration of the extra-framework content in alkali-poor beryl: A multi-methodological study," Am. Mineral. **91**, 29–34 (2006).
[25]P. A. Wood, F. H. Allen, and E. Pidcock, "Hydrogen-bond directionality at the donor H atom—analysis of interaction energies and database statistics," CrystEngComm **11**, 1563–1571 (2009).
[26]R. K. Pathria and P. D. Beale, "Formulation of quantum statistics," in *Statistical Mechanics* (Elsevier, 2011), pp. 115–140.
[27]V. G. Gueorguiev, A. R. P. Rau, and J. P. Draayer, "Confined one-dimensional harmonic oscillator as a two-mode system," Am. J. Phys. **74**, 394–403 (2006).
[28]A. I. Kolesnikov, L. M. Anovitz, E. Mamontov, A. Podlesnyak, and G. Ehlers, "Strong anisotropic dynamics of ultra-confined water," J. Phys. Chem. B **118**, 13414–13419 (2014).
[29]A. I. Kolesnikov, G. F. Reiter, T. R. Prisk, M. Krzystyniak, G. Romanelli, D. J. Wesolowski, and L. M. Anovitz, "Inelastic and deep inelastic neutron spectroscopy of water molecules under ultra-confinement," J. Phys.: Conf. Ser. **1055**, 012002 (2018).
[30]B. Kolesov, "Vibrational states of H_2O in beryl: Physical aspects," Phys. Chem. Miner. **35**, 271–278 (2008).
[31]B. P. Gorshunov, E. S. Zhukova, V. I. Torgashev, V. V. Lebedev, G. S. Shakurov, R. K. Kremer, E. V. Pestrjakov, V. G. Thomas, D. A. Fursenko, and M. Dressel, "Quantum behavior of water molecules confined to nanocavities in gemstones," J. Phys. Chem. Lett. **4**, 2015–2020 (2013).